

# Particle Dynamics Near Kerr-MOG Black Hole

M. Sharif <sup>\*</sup> and Misbah Shahzadi <sup>†</sup>

Department of Mathematics, University of the Punjab,  
Quaid-e-Azam Campus, Lahore-54590, Pakistan.

## Abstract

This paper explores the dynamics of both neutral as well as charged particles orbiting near a rotating black hole in scalar-tensor-vector gravity. We study the conditions for the particle to escape at the innermost stable circular orbit. We investigate stability of orbits through effective potential and Lyapunov exponent in the presence of magnetic field. The effective force acting on particle is also discussed. We also study the center of mass energy of particle collision near the horizon of this black hole. Finally, we compare our results with the particle motion around Schwarzschild, Kerr and Schwarzschild-MOG black holes. It is concluded that the external magnetic field, spin parameter as well as dimensionless parameter of the theory have strong effects on particle dynamics in modified gravity.

**Keywords:** Kerr-MOG BH; Magnetic field; Geodesics.

**PACS:** 04.50.Kd; 04.70.-s; 52.30.Cv; 52.25.Xz.

## 1 Introduction

Mysteries of the universe have always been an interesting topic for the physicists. Many cosmological observations indicate that the universe is facing

---

<sup>\*</sup>msharif.math@pu.edu.pk

<sup>†</sup>misbahshahzadi51@gmail.com

accelerated expansion which is believed due to the existence of mysterious form of energy named as dark energy. The matter which cannot be seen directly but can be observed by its gravitational effects on visible matter is known as dark matter (DM). This does not interact with electromagnetic force and light. Modified gravity theories help to uncover the enigmatic nature of dark energy and DM. These theories are constructed by modifying the matter or gravitational part of the Einstein-Hilbert action.

Modified theories with additional fields (scalar or vector) like scalar-tensor theories are the generalization of tensor theory (general relativity). In Brans-Dicke theory (example of scalar-tensor theories), gravitational field is obtained by tensor field  $R$  and massless scalar field  $\phi$ . The vector-tensor theories are formulated by adding a dynamical vector field coupled to gravity in the Einstein-Hilbert action. Moffat [1] formulated a modified theory of gravity (MOG) termed as scalar-tensor-vector gravity (STVG) which acts as an alternative of DM. This theory introduces new fields in general relativity which makes the gravitational field stronger. Its action consists of the usual Einstein-Hilbert term associated with the metric tensor  $g_{\mu\nu}$ , a massive vector field  $\phi_\mu$  and three scalar fields which represent the running values of gravitational constant  $G$ , coupling constant  $\omega$  (determines the coupling strength between matter and vector field) and the vector field's mass  $\mu$  (adjusts the coupling range). The scalar field  $G = G_N(1 + \alpha)$  is the strength of gravitational attraction, where  $G_N$  is Newton's gravitational constant and  $\alpha$  is a dimensionless parameter of the theory. The vector field produces a repulsive gravitational force which is related to a fifth force charge proportional to mass-energy. This theory helps to explain the solar system, rotational curves of galaxies, motion of galaxy clusters, gravitational lensing of galaxy and cluster of galaxies without DM [2].

Moffat and Toth [3] studied static spherically symmetric vacuum solutions for flat FRW model and also discussed the origin of inertia in STVG theory. Deng et al. [4] discussed the modifications of STVG and constraint on its parameters. Mishra and Singh [5] studied the galaxy rotational curves and compared the form of acceleration law in fourth order gravity with STVG as well as modified Newtonian dynamics. Moffat and Rahvar [6] used the weak-field approximation to test the dynamics of cluster of galaxies and found that this theory is consistent with the observational data from the solar system to megaparsec scales. Roshan [7] discussed some cosmological solutions for flat FRW model using Noether symmetry approach. Sharif and Yousaf [8] used this approach to find anisotropic exact solutions of locally

rotationally symmetric Bianchi type-I model. Mureika et al. [9] analyzed thermodynamics of Schwarzschild-MOG as well as Kerr-MOG black hole (BH) and found a change in entropy area law with the increase of parameter  $\alpha$ .

The dynamics of particles (neutral or charged, massive or massless) around BH is one of the most interesting problems in BH astrophysics. This plays a key role in understanding the geometrical structure of spacetime. New observational evidence for BHs provides new motivations for the investigation of general relativistic dynamics of particles and electromagnetic fields in the vicinity of BHs. Astronomical observations over the last decade indicate the existence of stellar-mass and supermassive BHs in some X-ray binary systems and in galactic centers.

Hussain and Jamil [10] studied timelike geodesics around Schwarzschild-MOG BH and found that the stability of orbits increases due to the presence of vector field in STVG theory. Pradhan [11] explored circular geodesics near a Kerr-Newman-Taub-NUT spacetime and found that the energy gain is maximum for zero NUT parameter and also for maximum spin value. Babar et al. [12] studied the motion of charged particles in the vicinity of weakly magnetized naked singularity and explored the escape velocity of particles orbiting in the inner most stable circular orbits (ISCOs). Soroushfar et al. [13] discussed the geodesics around charged rotating BH in  $f(R)$  gravity and found that the shape of an orbit depends on the value of energy, angular momentum, charge as well as cosmological constant. Sharif and Iftikhar [14] studied this phenomenon around a higher dimensional BH and found that higher dimensions have strong effects on particles motion.

Bardeen [15] investigated characteristics of Kerr BH and its circular orbits. Aliev and Ozdemir [16] discussed charged particles motion around rotating BH and found that magnetic field has strong effect to enlarge the region of stability close to the event horizon. Frolov and Stojkovic [17] explored particles motion around five-dimensional rotating BH and found that there does not exist SCOs in equatorial planes. Aliev and Gumrukcuoglu [18] studied charged rotating BHs on 3-brane and found that negative tidal charge increases the horizon radius as well as radii of photon orbit. Shiose et al. [19] investigated charged particles motion near a weakly magnetized rotating BH and found that the radius of ISCO increases due to increase of magnetic field. Amir et al. [20] studied particle dynamics near a rotating regular Hayward BH and showed that for particle having angular momentum  $L > L_c$  ( $L_c$  is critical angular momentum), geodesics never fall into the BH.

However, for  $L < L_c$ , the geodesics always fall into the BH and for  $L = L_c$ , the geodesics fall into the BH exactly at the event horizon.

The collision energy of particles in the center of mass frame (an inertial frame in which center of mass is at rest) that results in the formation of new particles is known as center of mass energy (CME). This depends upon the nature of colliding particles (e.g. charged or neutral), astrophysical object (BH or naked singularity) and gravitational field around the object. When the particles collision occurs near the horizon, the particles are blue-shifted due to infinite energy in CM frame [21]. Harada and Kimura [22] studied the particles collision in ISCO near Kerr BH and discussed the CME near the horizon. Sharif and Haider [23] investigated the CME for Demianski and Plebanski BHs without NUT parameter and examined the dependence of CME on the spin of BH. Sultana [24] discussed the collision of particles around a Kerr like BH in Brans-Dicke theory and found that CME is finite whether the BH is extremal or not. Armaza et al. [25] studied the spinning massive particles collision in the background of Schwarzschild BH and found that the CME increases due to the spin of BH.

In this paper, we discuss the dynamics of particles near a Kerr-MOG BH in the absence as well as presence of magnetic field. The paper is organized as follows. In section 2, we introduce Kerr-MOG BH and equations of motion of a neutral as well as charged particles. Section 3 explores the behavior of escape velocity, effective potential, effective force acting on the particles and instability of the orbits. In section 4, the CME for the colliding particles is discussed. In the last section, we summarize our results.

## 2 Dynamics of Particle

Here we explore the equations of motion for both neutral as well as charged particles around a Kerr-MOG BH.

### 2.1 Neutral Case

Kerr-MOG BH is the solution of MOG field equations and is fully described by the mass  $M$ , spin angular momentum  $J = Ma$  and parameter  $\alpha$ . The line element around a Kerr-MOG BH is given as [26]

$$ds^2 = -\frac{\Delta}{\rho^2} (dt - a \sin^2 \theta d\phi)^2 + \frac{\sin^2 \theta}{\rho^2} [(r^2 + a^2) d\phi - a dt]^2 + \frac{\rho^2}{\Delta} dr^2 + \rho^2 d\theta^2, \quad (1)$$

where

$$\Delta = r^2 + a^2 - 2GMr + \alpha G_N GM^2, \quad \rho^2 = r^2 + a^2 \cos^2 \theta.$$

Here,  $G$  is taken as the gravitational constant, the free parameter  $\alpha$  determines gravitational field strength and  $M$  is the mass of BH. The metric (1) is asymptotically flat, stationary and axially symmetric around  $z$ -axis. The Killing vectors corresponding to these symmetries are

$$\xi_{(t)}^\sigma \partial_\sigma = \partial_t, \quad \xi_{(\phi)}^\sigma \partial_\sigma = \partial_\phi,$$

where  $\xi_{(t)}^\sigma = (1, 0, 0, 0)$  and  $\xi_{(\phi)}^\sigma = (0, 0, 0, 1)$ . When  $\alpha = 0$ , the metric (1) reduces to the Kerr metric, further  $a = \alpha = 0$  leads to the Schwarzschild metric and for  $a = 0$ , we obtain Schwarzschild-MOG metric. The Kerr-MOG metric (1) is singular if  $\rho$  or  $\Delta$  vanishes. The curvature and coordinate singularities correspond to  $\rho = 0$  and  $\Delta = 0$ , respectively. The horizons of (1) can be obtained by  $\Delta = 0$  as

$$r_\pm = GM \pm \sqrt{G^2 M^2 - a^2 - \alpha G_N GM^2},$$

here  $\pm$  sign correspond to the event and Cauchy horizons, respectively. The ergosphere can be obtained by solving  $g_{tt} = 0$

$$r_{es} = GM \pm \sqrt{G^2 M^2 - \alpha G_N GM^2}.$$

For  $\theta = 0, \pi$ , both ergosphere and event horizon coincide. The extremal condition is located at  $G^2 M^2 = a^2 + \alpha G_N GM^2$ . The corresponding angular velocity is

$$\Omega_H = \frac{a}{(r_+^2 + a^2)} = \frac{a}{2G^2 M^2 - \alpha G_N GM^2 + 2GM\sqrt{G^2 M^2 - a^2 - \alpha G_N GM^2}}.$$

We consider the equatorial plane to find the motion of test particle, i.e,  $\theta = \frac{\pi}{2}$ ,  $\dot{\theta} = 0$ .

The motion of a neutral particle can be illustrated by the Lagrangian

$$\mathcal{L} = \frac{1}{2} g_{\sigma\eta} \dot{x}^\sigma \dot{x}^\eta,$$

where  $\dot{x}^\sigma = u^\sigma = \frac{dx^\sigma}{d\tau}$  is the four velocity of particle and  $\tau$  is the proper time. For Kerr-MOG BH, the Lagrangian becomes

$$2\mathcal{L} = - \left( \frac{r^2 - 2GMr + \alpha G_N GM^2}{r^2} \right) \dot{t}^2 - 2a \left( \frac{2GMr - \alpha G_N GM^2}{r^2} \right) \dot{t} \dot{\phi}$$

$$+ \frac{r^2}{\Delta} \dot{r}^2 + \frac{[r^2(r^2 + a^2) + a^2(2GMr - \alpha G_N GM^2)]}{r^2} \dot{\phi}^2. \quad (2)$$

It is clear from Eq.(2) that  $t$  and  $\phi$  are cyclic coordinates. Corresponding to these cyclic coordinates there are two constants of motion, i.e., total energy  $E$  and azimuthal angular momentum  $L_z$  which are conserved along geodesics. The generalized momenta are

$$\begin{aligned} -p_t &= -\left(\frac{r^2 - 2GMr + \alpha G_N GM^2}{r^2}\right) \dot{t} - a \left(\frac{2GMr - \alpha G_N GM^2}{r^2}\right) \dot{\phi} \\ &= E, \end{aligned} \quad (3)$$

$$\begin{aligned} p_\phi &= -a \left(\frac{2GMr - \alpha G_N GM^2}{r^2}\right) \dot{t} \\ &+ \frac{[r^2(r^2 + a^2) + a^2(2GMr - \alpha G_N GM^2)]}{r^2} \dot{\phi} = L_z, \end{aligned} \quad (4)$$

$$p_r = \frac{r^2}{\Delta} \dot{r},$$

where dot denotes derivative with respect to  $\tau$ . From Eqs.(3) and (4), we obtain

$$\begin{aligned} \dot{t} &= \frac{1}{r^2 \Delta} [(r^2(r^2 + a^2) + a^2(2GMr - \alpha G_N GM^2)) E \\ &- a L_z (2GMr - \alpha G_N GM^2)], \end{aligned} \quad (5)$$

$$\dot{\phi} = \frac{1}{r^2 \Delta} [(r^2 - 2GMr + \alpha G_N GM^2) L_z + a(2GMr - \alpha G_N GM^2) E] \quad (6)$$

The total angular momentum is given as

$$L^2 = (r^2 \dot{\theta})^2 + (r^2 \dot{\phi} \sin \theta)^2,$$

here  $v_\perp^2 \equiv -r\dot{\theta}_0$ ,  $\dot{\theta}_0$  is the initial angular velocity of the particle. Using the value of  $\dot{\phi}$  from Eq.(6), we have

$$\begin{aligned} L^2 &= \frac{[(r^2 - 2GMr + \alpha G_N GM^2) L_z + a(2GMr - \alpha G_N GM^2) E]^2}{(r^2 + a^2 - 2GMr + \alpha G_N GM^2)^2} \\ &+ r^2 v_\perp^2. \end{aligned} \quad (7)$$

Using the normalization condition,  $g_{\sigma\eta} u^\sigma u^\eta = -1$ , it follows that

$$\dot{r}^2 = E^2 + \frac{1}{r^2} (a^2 E^2 - L_z^2) + \frac{1}{r^4} (2GMr - \alpha G_N GM^2) (aE - L_z)^2 - \frac{\Delta}{r^2}. \quad (8)$$

Equations (5)-(8) are useful to discuss various features of particle motion near (1). From Eq.(8), we obtain

$$\frac{1}{2} (E^2 - 1) = \frac{1}{2} \dot{r}^2 + U_{eff}(r, E, L_z),$$

where

$$\begin{aligned} U_{eff}(r, E, L_z) &= \frac{-GM}{r} + \frac{[L_z^2 - a^2 (E^2 - 1) + \alpha G_N G M^2]}{2r^2} \\ &- \frac{GM}{r^3} (aE - L_z)^2 + \frac{\alpha G_N G M^2}{2r^4} (aE - L_z)^2. \end{aligned}$$

The maximum and minimum values of effective potential  $U_{eff}$  determine the unstable and stable circular orbits, respectively. The radius of innermost stable circular orbit ( $r_0$ ) can be found by solving  $\frac{dU_{eff}}{dr} = 0$ . We have solved  $\frac{dU_{eff}}{dr} = 0$  using Mathematica 8.0 and found three roots of  $r$ . We have ignored the two imaginary values of  $r$  and the rest is the radius of ISCO ( $r_0$ ). The energy and azimuthal angular momentum corresponding to  $r_0$  are

$$\begin{aligned} E_0 &= \frac{1}{r_0} \left[ \frac{r_0^2 - 2GM r_0 + \alpha G_N G M^2 \mp a \sqrt{GM(r_0 - M\alpha G_N)}}{\sqrt{r_0^2 - 3GM r_0 + 2\alpha G_N G M^2 \mp 2a \sqrt{GM(r_0 - M\alpha G_N)}}} \right], (9) \\ L_{z0} &= \frac{1}{r_0^2} \left[ \mp \sqrt{GM(r_0 - M\alpha G_N)} (a^2 + r_0^2 \pm 2a \sqrt{GM(r_0 - M\alpha G_N)}) \right. \\ &- \alpha G_N G M^2 a \left. \left[ r_0^2 - 3GM r_0 + 2\alpha G_N G M^2 \right. \right. \\ &\left. \mp 2a \sqrt{GM(r_0 - M\alpha G_N)} \right]^{-\frac{1}{2}}, \end{aligned} \quad (10)$$

where  $r_0$  is the radius of ISCO and  $\pm$  signs correspond to the counter-rotating and co-rotating orbits, respectively. For  $\alpha = 0$ , Eqs.(9) and (10) reduce to Kerr-BH [27].

Consider a particle orbiting in ISCO colliding with another particle which is at rest. After collision, there are three cases (depending upon the collision process) for the particles motion, i.e, either captured by BH, or bounded near a BH or escape to infinity. If there is a small change in energy and angular momentum then the particle's orbit will slightly be perturbed and particle remains bounded. But for large change, it may be captured by BH or escape to infinity. After collision, particle will be in new plane with respect to

the original equatorial plane. Thus the particle would have new energy and azimuthal angular momentum. For simplicity, we assume that, after collision, initial radial velocity and azimuthal angular momentum do not change and particle attains escape velocity  $v_{esc}$  orthogonal to the equatorial plane. The new energy and angular momentum of particle are

$$\begin{aligned}
L_{new}^2 &= r_0^2 v_\perp^2 + \frac{[(r_0^2 - 2GM r_0 + \alpha G_N G M^2) L_{z0} + a(2GM r_0 - \alpha G_N G M^2) E_0]^2}{(r_0^2 + a^2 - 2GM r_0 + \alpha G_N G M^2)^2}, \\
E_{new}^2 &= 1 - \frac{2GM}{r_0} + \frac{[L_{z0}^2 - a^2(E_0^2 - 1) + \alpha G_N G M^2]}{r_0^2} - \frac{2GM}{r_0^3} (aE_0 - L_{z0})^2 \\
&\quad + \frac{\alpha G_N G M^2}{r_0^4} (aE_0 - L_{z0})^2.
\end{aligned} \tag{11}$$

After collision, particle attains greater energy and angular momentum as compared to before collision. We observe from the above equation that  $E_{new} \rightarrow 1$  as  $r_0 \rightarrow \infty$ . Thus for unbounded motion, particle requires  $E_{new} \geq 1$  to escape, whereas particle cannot escape for  $E_{new} < 1$ .

## 2.2 Charged Case

The theoretical and experimental evidences indicate that magnetic field must be present in the vicinity of BHs. It arises due to plasma in the surrounding of BH [28] and plays an important role in the formation, structure and evolution of planets, stars, galaxies and possibly the entire universe [29]. The magnetic field has strong effects around the event horizon but does not change the geometry of BH rather the motion of charged particles is affected [30]. We assume that a particle has an electric charge and its motion is affected by magnetic field in the BH exterior. Since Kerr-MOG BH is non-vacuum, so we follow [31] to calculate the four-vector potential given as

$$\begin{aligned}
A^\sigma &= \left[ \frac{-Qr}{r^2 - 2f} + a\check{B} \left( 1 + \frac{f_2 \sin^2 \theta}{r^2} \right) \right] \xi_{(t)}^\sigma + \left[ \frac{\check{B}}{2} \left( 1 + \frac{2f_2}{r^2} \right) \right. \\
&\quad \left. - \frac{Qa}{r(r^2 - 2f)} \right] \xi_{(\phi)}^\sigma,
\end{aligned}$$

where  $f = f_1 r + f_2$  with  $f_1, f_2$  are constants and  $\check{B}$  is the magnetic field. For simplicity, we take  $Q = 0$  and also for the equatorial plane  $\theta = \pi/2$ . Thus



the above equation becomes

$$A^\sigma = a\check{B} \left(1 + \frac{f_2}{r^2}\right) \xi_{(t)}^\sigma + \frac{\check{B}}{2} \left(1 + \frac{2f_2}{r^2}\right) \xi_{(\phi)}^\sigma.$$

For (1), the above equation takes the form

$$A^\sigma = a\check{B} \left(1 - \frac{\alpha G_N G M^2}{2r^2}\right) \xi_{(t)}^\sigma + \frac{\check{B}}{2} \left(1 - \frac{\alpha G_N G M^2}{r^2}\right) \xi_{(\phi)}^\sigma.$$

The magnetic field for an observer having four velocity  $u_\eta$  is defined as

$$\check{B}^\sigma = -\frac{1}{2} e^{\sigma\eta\gamma\delta} F_{\gamma\delta} u_\eta,$$

where  $e^{\sigma\eta\gamma\delta} = \frac{\varepsilon^{\sigma\eta\gamma\delta}}{\sqrt{-g}}$  and  $\varepsilon^{\sigma\eta\gamma\delta}$  is the Levi-Civita symbol,  $g = \det(g_{\sigma\eta})$  and  $\varepsilon_{0123} = 1$ . The Maxwell field tensor is  $F_{\sigma\eta} = A_{\eta;\sigma} - A_{\sigma;\eta}$ .

The Lagrangian of a particle having electric charge  $q$  and mass  $m$  is

$$\mathcal{L} = \frac{1}{2} g_{\sigma\eta} u^\sigma u^\eta + \frac{q}{m} A_\sigma u^\sigma.$$

The generalized four momentum is given by

$$p_\sigma = m u_\sigma + q A_\sigma.$$

In the presence of magnetic field, the constants of motion are

$$\begin{aligned} \dot{t} &= \frac{1}{r^3 \Delta} [r(8a^3 B G^2 M^2 - 2aG(2a^2 B - aE + L)Mr + a^2(-2aB + E) \\ &\times r^2 + (-2aB + E)r^4) + a\alpha G_N G M^2(-aEr + a^2 B(-4GM + 3r) \\ &+ r(L + Br(2GM + r)) - Br\alpha G_N G M^2)], \end{aligned} \quad (12)$$

$$\begin{aligned} \dot{\phi} &= \frac{1}{r^3 \Delta} [r(2aEGMr + a^2 B(8G^2 M^2 - 8GMr + r^2) - (2GMr - r)r \\ &\times (L + Br^2)) + \alpha G_N G M^2(-aEr + a^2 B(-4GM + 3r) + r(L + 2B \\ &\times GMr) - Br\alpha G_N G M^2)], \end{aligned} \quad (13)$$

where  $B = \frac{q\check{B}}{2m}$ . Using the normalization condition, we obtain

$$\dot{r}^2 r^6 = [r(a^4 B^2(4GM - 3r)(8G^2 M^2 - 6GMr - r^2) - 4a^3 BEr(-4G^2 M^2$$

$$\begin{aligned}
& + 2GMr + r^2) - 4aEr^2(GLM + Br^3) + a^2r(-2BL(8G^2M^2 - 8G \\
& \times Mr + r^2) + 2B^2r^2(-6G^2M^2 + 4GMr + r^2) + r(-r + E^2(2GM \\
& + r))) + r^2(-L^2r + (-1 + E^2 - 2BL)r^3 - B^2r^5 + 2GM(r^2 + (L \\
& + Br^2)^2))) - \alpha G_N GM^2(16a^4B^2G^2M^2 - 8a^2BG(3a^2B - aE + L) \\
& \times Mr + ((3a^2B - aE + L)^2 - 16a^2B^2G^2M^2)r^2 + 4BG(2a^2B - a \\
& \times E + L)Mr^3 + (1 + 2aB(2aB - E))r^4 + 4B^2GMr^5 - B^2r^6 + Br \\
& \times \alpha G_N GM^2(a^2B(8GM - 6r) + 2aEr - r(2L + Br(2GM + r)) \\
& + Br\alpha G_N GM^2))] , \tag{14}
\end{aligned}$$

which can be written as

$$\frac{1}{2} (E^2 - 1) = \frac{1}{2} \dot{r}^2 + U_{eff}(r, E, L_z, B),$$

where

$$\begin{aligned}
U_{eff}(r, E, L_z, B) &= \frac{-1}{2r^6} [r(a^4B^2(4GM - 3r)(8G^2M^2 - 6GMr - r^2) - 4a^3 \\
& \times BEr(-4G^2M^2 + 2GMr + r^2) - 4aEr^2(GL_zM + Br^3) \\
& + a^2r(-2BL_z(8G^2M^2 - 8GMr + r^2) + 2B^2r^2(-6G^2M^2 \\
& + 4GMr + r^2) + r(-r + E^2(2GM + r))) + r^2(-L_z^2r - 2 \\
& \times BL_zr^3 - B^2r^5 + 2GM(r^2 + (L_z + Br^2)^2))) - \alpha G_N GM^2 \\
& \times (16a^4B^2G^2M^2 - 8a^2BG(3a^2B - aE + L_z)Mr + ((3a^2B \\
& - aE + L_z)^2 - 16a^2B^2G^2M^2)r^2 + 4BG(2a^2B - aE + L_z) \\
& \times Mr^3 + (1 + 2aB(2aB - E))r^4 + 4B^2GMr^5 - B^2r^6 + B \\
& \times r\alpha G_N GM^2(a^2B(8GM - 6r) + 2aEr - r(2L_z + Br(2G \\
& \times M + r)) + Br\alpha G_N GM^2))] . \tag{15}
\end{aligned}$$

Equations (12) to (15) are invariant under the transformations  $\phi \rightarrow -\phi, L_z \rightarrow -L_z, B \rightarrow -B$ .

### 3 Escape Velocity and Effective Potential

In this section, we discuss properties of the escape velocity and effective potential of a particle when  $G = 1, M = 1, G_N = 1, E = 1$ . Figure 1 shows the escape velocity for a particle moving around Kerr-MOG BH in

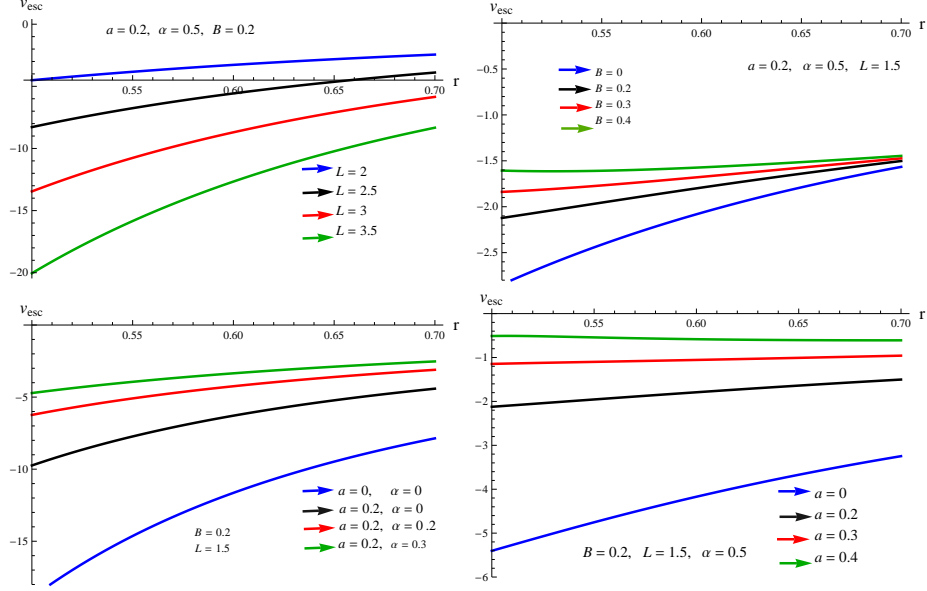


Figure 1: Escape velocity against  $r$ .

the presence of magnetic field. In the upper panel, the left graph indicates that particles with large angular momentum have less possibilities to escape as compared to those having small angular momentum. The right graph shows that the escape velocity increases with the increase of magnetic field. Particles attain more energy due to large values of magnetic field and can easily escape. In the lower panel, the left graph provides comparison for escape velocity of the Kerr-MOG BH with Schwarzschild and Kerr BHs. This shows that the Kerr-MOG BH has more  $v_{esc}$  as compared to Schwarzschild and Schwarzschild-MOG BH, also  $v_{esc}$  increases with increasing value of parameter  $\alpha$ .

The effect of spin on escape velocity is shown in the right graph. This also provides the comparison of escape velocity of particle around Schwarzschild-MOG BH with Kerr-MOG BH. We see that with the increase of spin of BH, particles have more possibilities to escape as  $v_{esc}$  is high for large values of spin parameter  $a$ . A rotating BH ( $a \neq 0$ ) may provide sufficient amount of energy to particle due to which it can escape to infinity as compared to non-rotating BH. It is also noted that particles in the vicinity of Schwarzschild-MOG BH can escape easily as compared to Kerr-MOG BH. We conclude that  $v_{esc}$  becomes almost constant as particle moves away from the BH.

Figure 2 shows the behavior of  $U_{eff}$  against  $r$ . The stable and unstable circular orbits correspond to minimum and maximum values of effective potential, respectively. In the upper panel, the left graph shows that initially orbits are unstable and then become stable, stability increases with the increase of  $L$ . The right graph is plotted for different values of  $B$ . We observe that the orbits are initially stable, then becomes unstable and stability decreases for increasing value of  $B$ . In the lower panel, the left graph shows that the particle motion becomes more unstable for high values of  $\alpha$ . The right graph indicates that circular orbits for Kerr-MOG BH are more unstable as compared to Kerr and Schwarzschild BH. The last graph is plotted for different values of spin parameter  $a$  which indicate that the stability of circular orbits decreases with the increase of  $a$ . Thus the motion of particle will be more unstable for large value of  $a$ . We note that circular orbits around Schwarzschild-MOG BH are more stable as compared to Kerr-MOG BH.

### 3.1 Effective Force

The effective force acting on particle provides the information about motion, i.e., whether it is attracted towards the BH or moving away from it [32]. We study the particle motion in the background of Kerr-MOG BH where attractive as well as repulsive gravitational forces can be produced by STVG. Here, we find the effective force acting on particle using Eq.(15) as [33]

$$\begin{aligned}
F &= \frac{-1}{2} \frac{dU_{eff}}{dr} \\
&= \frac{-GM}{2r^4} [L(3L + Br^2 - 6aE + 24a^2B) + 3a^2E^2 - 12a^3BE + 21a^4B^2 \\
&\quad - B^2r^4 + r^2 + 4a^2B^2r^2] - \frac{(\alpha G_N GM^2)^2}{2r^5} [4BL - 4aBE + B^2 + 12a^2B^2] \\
&\quad - \frac{(\alpha G_N GM^2)(GM)}{r^6} [BL(10a^2 - 3r^2) - B^2r^4 - 3aBEr^2 + 6a^2B^2r^2 + 10 \\
&\quad \times a^3BE - 30a^4B^2] - \frac{(\alpha G_N GM^2)^3}{r^6} 40a^4B^2 + \frac{(GM)^2}{r^5} [16a^2BL + 48a^4B^2 \\
&\quad - 16a^3BE + 6a^2B^2r^2] + \frac{\alpha G_N GM^2}{2r^5} [2L(L - 2aE + 6a^2B) + r^2 + 4a^2B^2r^2 \\
&\quad - 2aBEr^2 + 2a^2E^2 - 12a^3B + 18a^4B^2] + \frac{1}{2r^3} [L(1 + 2a^2B) + a^2 - 3a^4 \\
&\quad \times B^2 + 4a^3BE - a^2E^2 - B^2r^4] + \frac{(\alpha G_N GM^2)^3 B^2}{r^5} + \frac{(\alpha G_N GM^2)^2 (GM)}{2r^6}
\end{aligned}$$

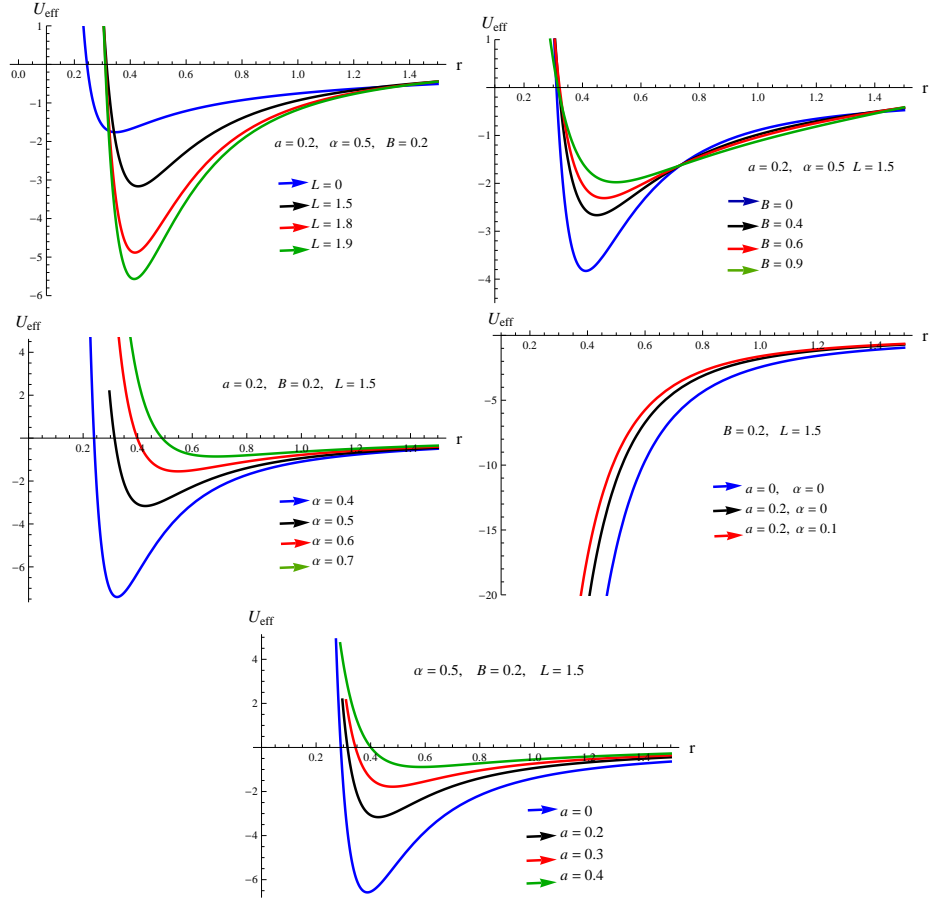


Figure 2: Effective potential versus  $r$ .

$$\times [20a^2B^2 - 3B^2r^2] + \frac{(\alpha G_N G M^2)(GM)^2}{r^7} [27a^4B^2 - 16a^2B^2r^2].$$

We see that the first, second and third terms are attractive if  $L(3L + Br^2 - 6aE + 24a^2B) > 3a^2E^2 - 12a^3BE + 21a^4B^2 - B^2r^4 + r^2 + 4a^2B^2r^2$ ,  $4BL > -4aBE + B^2 + 12a^2B^2$  and  $BL(10a^2 - 3r^2) > -B^2r^4 - 3aBEr^2 + 6a^2B^2r^2 + 10a^3BE - 30a^4B^2$ , respectively. The fourth term is also attractive. The fifth, sixth and seventh terms are repulsive if  $16a^2BL > 48a^4B^2 - 16a^3BE + 6a^2B^2r^2$ ,  $2L(L - 2aE + 6a^2B) > r^2 + 4a^2B^2r^2 - 2aBEr^2 + 2a^2E^2 - 12a^3B + 18a^4B^2$  and  $L(1 + 2a^2B) > a^2 - 3a^4B^2 + 4a^3BE - a^2E^2 - B^2r^4$ , respectively. The last three terms are also repulsive.

Figure 3 describes the behavior of effective force as a function of  $r$ . In the upper panel, the left graph shows that the effective force acting on particles is more attractive for large values of magnetic field. The right graph shows the comparison of effective force acting on a particle around Kerr-MOG BH with the Kerr and Schwarzschild BHs. We see that the effective force on a particle for Kerr-MOG BH attains more values than the Kerr and Schwarzschild BHs and increases for increasing value of  $\alpha$ . This means that repulsion to reach the singularity for Kerr-MOG BH is more as compared to that in Schwarzschild and Kerr BHs. The behavior of effective force for different values of spin parameter is represented in lower graph showing that effective force acting on particles increases with the increase of spin parameter and becomes almost constant as the particle moves away from the BH. It is also observed that effective force on particles in the vicinity of Schwarzschild-MOG BH is small as compared to the Kerr-MOG BH.

## 3.2 Lyapunov Exponent

Lyapunov exponent measures the average rate of expansion or contraction of trajectories in a phase space. The positive and negative Lyapunov exponents indicate divergence and convergence between neighboring orbits [34]. Using Eq.(15), we can find the Lyapunov exponent as [35]

$$\begin{aligned} \lambda &= \sqrt{\frac{-U''_{eff}(r_0)}{2\dot{t}^2(r_0)}} \\ &= \left[ \frac{1}{2L^2r^8} [(r(-2GM + r) + \alpha G_N G M^2)(r(-480a^4B^2G^3M^3 + 160a^2BG^2 \right. \\ &\quad \times (3a^2B - aE + L)M^2r - 12G(7a^4B^2 - 4a^3BE - 2aEL + L^2 + a^2(E^2 \end{aligned}$$

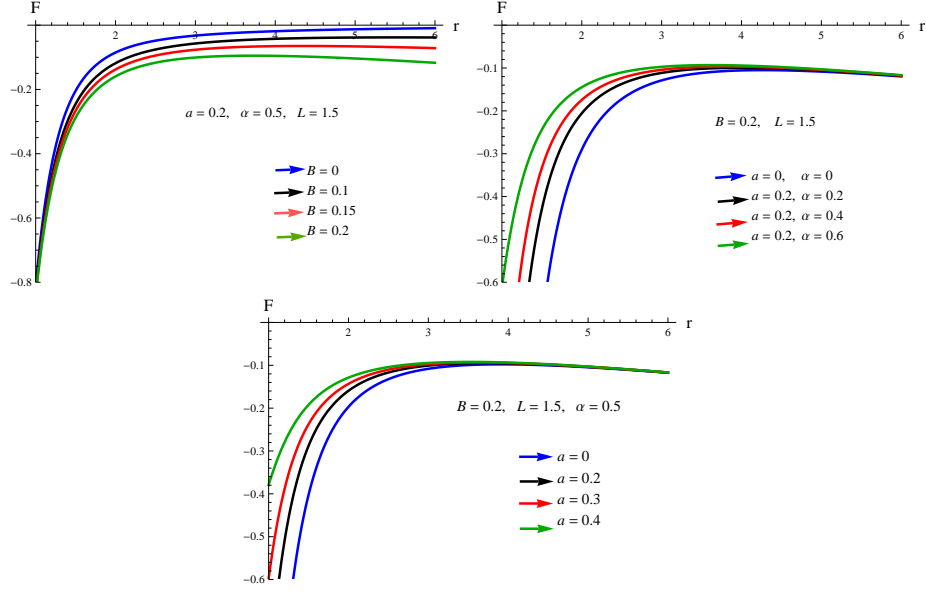


Figure 3: Effective force as a function of  $r$ .

$$\begin{aligned}
& + 8BL))Mr^2 + 3(-3a^4B^2 + 4a^3BE + L^2 + a^2(1 - E^2 + 2B(L + 6BG^2 \\
& \times M^2)))r^3 - 2G(1 + 2B(2a^2B + L))Mr^4 + B^2r^7) + \alpha G_N GM^2(336a^4B^2 \\
& \times G^2M^2 - 120a^2BG(3a^2B - aE + L)Mr + 10((3a^2B - aE + L)^2 - 16a^2 \\
& \times B^2G^2M^2)r^2 + 24BG(2a^2B - aE + L)Mr^3 + 3(1 + 2aB(2aB - E))r^4 \\
& + 4B^2GMr^5 + Br\alpha G_N GM^2(60a^2B(2GM - r) + 20aEr - r(20L + 3Br \\
& \times (4GM + r)) + 10Br\alpha G_N GM^2)))\Big]^{\frac{1}{2}} \Big|_{r=r_0} .
\end{aligned}$$

Figure 4 shows the graph of Lyapunov exponent as a function of  $B$ . In the upper panel, the left graph indicates that Lyapunov exponent has decreasing behavior for higher values of angular momentum representing that orbits are more unstable for small value of angular momentum as compared to large. The right graph gives a comparison for Kerr-MOG BH with the Kerr, Schwarzschild and Schwarzschild-MOG BHs. This shows that for Kerr-MOG BH, instability of circular orbits is higher as compared to Kerr, Schwarzschild and Schwarzschild-MOG BHs and instability increases with the increase of  $\alpha$ . The behavior of Lyapunov exponent for different values of spin parameter is shown in the lower graph. It is noted that orbits are more unstable with large value of  $a$  as compared to small.

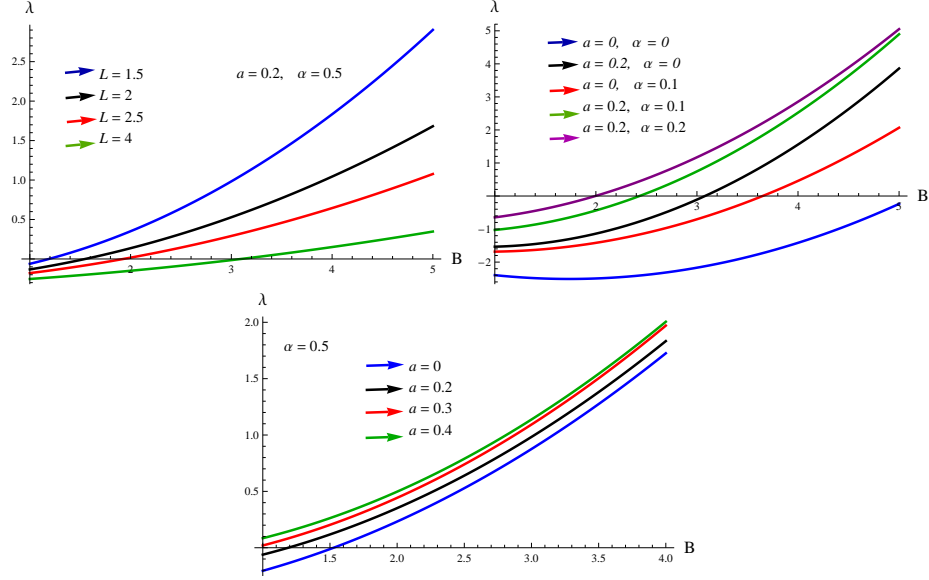


Figure 4: Lyapunov exponent as a function of  $B$  for  $L = 1.5$ .

## 4 Center of Mass Energy

The center of mass energy of two colliding particles can be obtained by adding their masses and kinetic energies depending upon the interacting particles and gravitational field around the astrophysical object. It is interesting to discuss the particle collision as it is a naturally occurring process in the universe. In the following, we discuss CME for neutral as well as charged particles.

### 4.1 Neutral Case

Let us consider two neutral particles with the same rest-mass  $m_0$  but different four velocities  $u_1^\sigma$  and  $u_2^\eta$  colliding with each other. The conserved energy and angular momentum of colliding particles are  $E_1$ ,  $E_2$ ,  $L_1$  and  $L_2$ . The CME of colliding particles is defined as

$$\left( \frac{E_{cm}}{\sqrt{2}m_0} \right)^2 = 1 - g_{\sigma\eta} u_1^\sigma u_2^\eta. \quad (16)$$



Inserting the values of  $g_{\sigma\eta}$ ,  $u_1^\sigma$  and  $u_2^\eta$  from Eqs.(5)-(8), the CME becomes

$$\begin{aligned} \left(\frac{E_{cm}}{\sqrt{2}m_0}\right)^2 &= \frac{1}{r^2\Delta}[(r(r(a^2 + r(-2GM + r)) + (r^3 + a^2(2GM + r))E_1E_2 \\ &- 2aGME_1L_2 - L_1(2aGME_2 + (r - 2MG)L_2) + \alpha G_N GM^2(r^2 \\ &- a^2E_1E_2 + L_1(aE_2 - L_2) + aE_1L_2)) - \sqrt{S_1S_2}], \end{aligned} \quad (17)$$

where

$$\begin{aligned} S_i &= r^4E_i^2 + r^2(a^2E_i^2 - L_i^2) + (2GMr - \alpha G_N GM^2) \\ &\times (aE_i - L_i)^2 - \frac{\Delta}{r^2}, \quad i = 1, 2. \end{aligned}$$

For  $a = \alpha = 0$  and  $\alpha = 0$ , Eq.(17) reduces to Schwarzschild and Kerr BHs, respectively [21].

## 4.2 Charged Case

Here we consider particles collision in the vicinity of magnetic field. In this case, the CME takes the following form

$$\begin{aligned} \left(\frac{E_{cm}}{\sqrt{2}m_0}\right)^2 &= \frac{1}{r^4\Delta}[-B^2G^3M^6r^2\alpha^3G_N^3 + BG^2M^4r\alpha^2G_N^2(-8a^2BGM + 6a^2B \\ &\times r + 2BGMr^2 + Br^3 - ar(E_1 + E_2) + r(L_1 + L_2)) + \alpha G_N GM^2 \\ &\times (-16a^4B^2G^2M^2 + 24a^4B^2GMr - 9a^4B^2r^2 + 16a^2B^2G^2M^2r^2 \\ &- 8a^2B^2GMr^3 + r^4 - 4a^2B^2r^4 - 4B^2GMr^5 + B^2r^6 + (E_1 + E_2) \\ &\times (-4a^3BGMr + 3a^3Br^2 + 2aBGMr^3 + aBr^4) + r(a^2B(4GM \\ &- 3r) - 2BGMr^2 + arE_1)L_2 + rL_1(a^2B(4GM - 3r) - 2BGMr^2 \\ &+ arE_2 - rL_2)) - r(-32a^4B^2G^3M^3 + 48a^4B^2G^2M^2r - 14a^4B^2G \\ &\times Mr^2 - a^2r^3 - 3a^4B^2r^3 + 12a^2B^2G^2M^2r^3 + 2GMr^4 - 8a^2B^2GM \\ &\times r^4 - r^5 - 2a^2B^2r^5 - 2B^2GMr^6 + B^2r^7 + (E_1 + E_2)(-8a^3BG^2M^2 \\ &\times r + 4a^3BGMr^2 + 2a^3Br^3 + 2aBr^5) + E_1E_2(-a^2r^2 - a^2r^3 - r^5 \\ &- 2a^2GMr^2) + r(Br^3(-2GM + r) + a^2B(8G^2M^2 - 8GMr + r^2) \\ &+ 2aGMrE_1)L_2 + rL_1(Br^3(-2GM + r) + a^2B(8G^2M^2 - 8GMr \\ &+ r^2) + 2aGMrE_2 + r(-2GM + r)L_2)) - \sqrt{S_1S_2}], \end{aligned}$$

where

$$\begin{aligned}
S_i = & [r(a^4 B^2(4GM - 3r)(8G^2 M^2 - 6GMr - r^2) - 4a^3 B E_i r(-4G^2 M^2 \\
& + 2GMr + r^2) - 4a E_i r^2(G L_i M + B r^3) + a^2 r(-2B L_i(8G^2 M^2 - 8GMr \\
& + r^2) + 2B^2 r^2(-6G^2 M^2 + 4GMr + r^2) + r(-r + E_i^2(2GM + r))) + r^2 \\
& \times (-L_i^2 r + (-1 + E_i^2 - 2B L_i)r^3 - B^2 r^5 + 2GM(r^2 + (L_i + B r^2)^2))) \\
& - \alpha G_N G M^2(16a^4 B^2 G^2 M^2 - 8a^2 B G(3a^2 B - a E_i + L_i)Mr + ((3a^2 B \\
& - a E_i + L_i)^2 - 16a^2 B^2 G^2 M^2)r^2 + 4B G(2a^2 B - a E_i + L_i)Mr^3 + (1 \\
& + 2a B(2a B - E_i))r^4 + 4B^2 G M r^5 - B^2 r^6 + B r \alpha G_N G M^2(a^2 B(8GM \\
& - 6r) + 2a E_i r - r(2L_i + B r(2GM + r)) + B r \alpha G_N G M^2))].
\end{aligned}$$

Clearly, the CME will be infinite if one of the colliding particles have diverging angular momentum at horizon. Thus, for finite CME only finite values of angular momentum are allowed. The behavior of CME as a function of  $r$  in the absence as well presence of magnetic field is depicted in Figure 5. In the upper panel, the left graph gives a comparison of CME for colliding particle near Kerr-MOG with Schwarzschild and Kerr BH. The collision occurring near the horizon of Kerr-MOG BH can produce high energy as compared to Schwarzschild and Kerr BHs and increases with the increase of parameter  $\alpha$ . The right graph is plotted for different values of spin parameter. We see that CME strongly depends on the rotation of BH. High energy can be achieved with the maximum spin. The CME for different values of parameter  $\alpha$  (left) and spin parameter (right) in the presence of magnetic field is shown in the lower panel. It is noted that maximum CME can be produced in the presence of magnetic field as compared to its absence. The CME has decreasing behavior with the increase of radial distance  $r$  and becomes almost constant away from the event horizon of BH. The CME for colliding particles does not diverge in the absence/presence of magnetic field.

Figure 6 is depicted for different values of  $L_1$  in the presence as well absence of magnetic field. We see that the CME decreases with the increase of angular momentum. The particle colliding with small angular momentum can produce high energy as compared to particle with large angular momentum. Initially, CME decreases and then becomes constant with the increase of radial distance  $r$ . It is also observed that CME is finite for finite values of angular momentum and attain more energy in the presence of magnetic field as compared to absence.

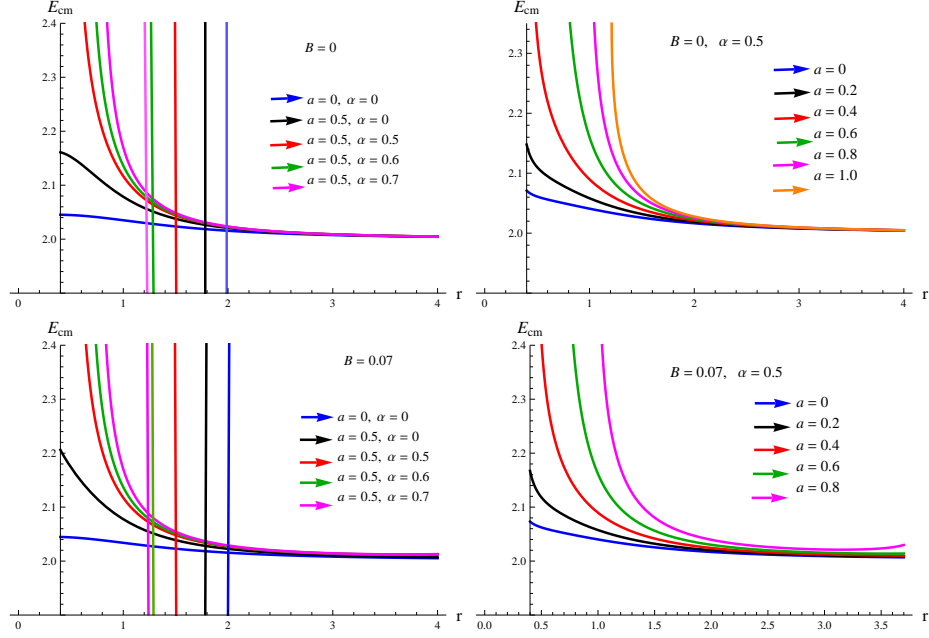


Figure 5: The CME with respect to  $r$  for  $L_1 = 1$  and  $L_2 = 1.5$ . Here, the vertical lines are event horizons.

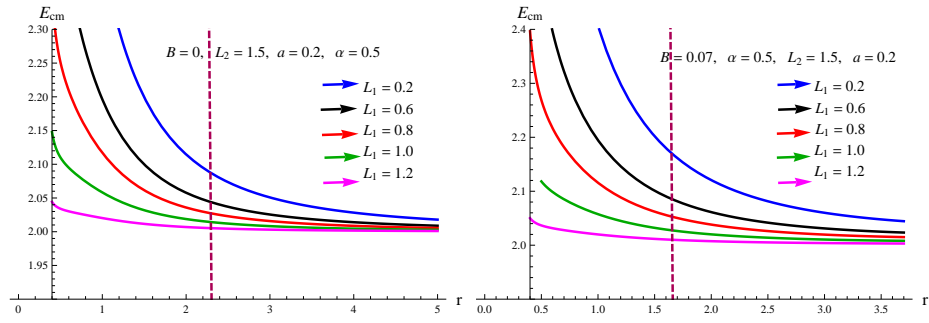


Figure 6: The CME as a function of  $r$ . The vertical line represent the event horizon.

## 5 Concluding Remarks

In this paper, we have studied the dynamics of particles around the Kerr-MOG BH in the absence/presence of magnetic field. We have explored geodesics for both neutral as well as charged particles. We have graphically discussed conditions for a particle to escape to infinity after its collision with another particle. The effect of magnetic field, angular momentum, parameter  $\alpha$  as well as spin parameter  $a$  on the motion of neutral and charged particles is also analyzed graphically. It is seen that the escape velocity increases with the increase of  $\alpha$  and magnetic field but decreases with the increase of  $L$ . The particles can attain more energy in the presence of magnetic field and can escape easily. The escape velocity also depends upon the spin of BH. There will be more possibilities to escape to infinity for large value of spin parameter. It is found that the escape velocity of particle around Schwarzschild BH is smaller as compared to Kerr and Kerr-MOG BH. Particles cannot escape easily in the vicinity of Kerr-MOG BH as compared to Kerr, Schwarzschild and Schwarzschild-MOG BHs.

We have explored stability of circular orbits by the effective potential. It is observed that the effective potential increases for large values of magnetic field which indicates that the presence of magnetic field increases the stability of particles orbits. We have compared the stability of circular orbits around Kerr-MOG BH with the Kerr and Schwarzschild BHs which indicates that circular orbits around Kerr-MOG BH are more unstable as compared to Kerr, Schwarzschild and Schwarzschild-MOG BHs. We note that large magnetic field leads to unstable motion. The rotation of BH have strong effects on the stability of orbits which decreases with the increase of  $a$ . We have also discussed the instability of circular orbits through Lyapunov exponent as a function of magnetic field  $B$ .

Finally, we have calculated the CME for two interacting particles around the Kerr-MOG BH. It is found that particle collision can produce high energy near Kerr-MOG BH as compared to Kerr, Schwarzschild and Schwarzschild-MOG BHs. We observe that the CME increases with the increase of spin parameter as well as parameter  $\alpha$  but decreases with the increase of angular momentum. The CME is finite for finite values of angular momentum and can be infinite for diverging angular momentum. We conclude that the external magnetic field, parameter  $\alpha$ , spin parameter affect the motion of particles in STVG. It is worth mentioning here that, our work is the generalization of [10] reduce to Schwarzschild-MOG BH [10] when  $a = 0$  and to Schwarzschild

BH [36] for  $a = \alpha = 0$ .

## References

- [1] Moffat, J.W.: J. Cosmol. Astropart. Phys. **03**(2006)004.
- [2] Moffat, J.W.: Int. J. Mod. Phys. D **16**(2007)2075.
- [3] Moffat, J.W. and Toth, V.T.: Class. Quantum Grav. **26**(2009)085002; Mon. Not. R. Astron. Soc. **395**(2009)25.
- [4] Deng, X.M., Xie, Y. and Huang, T.Y.: Phys. Rev. D **79**(2009)044014.
- [5] Mishra, P. and Singh, T.P.: Phys. Rev. D **88**(2013)104036.
- [6] Moffat, J.W. and Rahvar, S.: Mon. Not. R. Astron. Soc. **441**(2014)3724.
- [7] Roshan, M.: Eur. Phys. J. C **75**(2015)405.
- [8] Sharif, M. and Yousaf, A.: Eur. Phys. J. Plus **131**(2016)307.
- [9] Mureika, J.R., Moffat, J.W. and Faizal, M.: Phys. Lett. B **757**(2016)528.
- [10] Hussain, S. and Jamil, M.: Phys. Rev. D **92**(2015)043008.
- [11] Pradhan, P.: Class. Quantum Grav. **32**(2015)165001.
- [12] Babar, G.Z., Jamil, M. and Lim, Y.K.: Int. J. Mod. Phys. D **25**(2016)1650024.
- [13] Soroushfar, S. et al.: Phys. Rev. D **94**(2016)024052.
- [14] Sharif, M. and Iftikhar, S.: Eur. Phys. J. C **76**(2016)404.
- [15] Bardeen, J.M.: Astrophys. J. **178**(1972)347.
- [16] Aliev, A.N. and Ozdemir, N.: Mon. Not. R. Astron. Soc. **336**(2002)241.
- [17] Frolov, V. and Stojkovic, D.: Phys. Rev. D **68**(2003)064011.
- [18] Aliev, A. N. and Gumrukcuoglu, A. E.: Phys. Rev. D **71**(2005)104027.
- [19] Shiose, R., Kimura, M. and Chiba, T.: Phys. Rev. D **90**(2014)124016.

- [20] Amir, M., Ahmed, F. and Ghosh, S.G.: Eur. Phys. J. C **76**(2016)532.
- [21] Banados, M., Silk, J. and West, S. M.: Phys. Rev. Lett. **103**(2009)111102.
- [22] Harada, T. and Kimura, M.: Phys. Rev. D **83**(2011)084041.
- [23] Sharif, M. and Haider, N.: Astrophys. Space Sci. **346**(2013)111.
- [24] Sultana, J.: Phys. Rev. D **92**(2015)104022.
- [25] Armaza, C., Banados, M. and Koch, B.: Class. Quantum Grav. **33**(2016)105014.
- [26] Moffat, J.W.: Eur. Phys. J. C **75**(2015)175.
- [27] Chandrasekhar, S.: *The Mathematical Theory of Black Holes* (Oxford University Press, 1983); Hobson, M.P., Efstathiou, G.P. and Lasenby, A.N.: *General Relativity* (Cambridge University Press, 2006).
- [28] Borm, C.V. and Spaans, M.: Astron. Astrophys. **553**(2013)L9.
- [29] Dobbie, P.B., Kuncic, Z., Bicknell, G.V., Salmeron, R. Proceedings of IAU Symposium 259 Galaxies (Tenerife, 2008)
- [30] Znajek, R.: Nature 262(1976)270; Blandford, R.D. and Znajek, R.L.: Mon. Not. R. Astron. Soc. **179**(1977)433.
- [31] Azreg-Anou, M.: Eur. Phys. J. C **76**(2016)414.
- [32] Routh, E.J.: *A Treatise On Dynamics Of A Particle* (CUP Archive, 1898).
- [33] Fernando, S.: Gen. Relativ. Gravit. **44**(2012)1857.
- [34] Wu, X. and Huang, T.Y.: Phys. Lett. A **313**(2003)77.
- [35] Cardoso, V. et al.: Phys. Rev. D **79**(2009)064016.
- [36] Frolov, V.P. and Shoom, A.A.: Phys. Rev. D **82**(2010)084034.